The Pliocene thrust system of the Gran Sasso salient (Central Apennines, Italy)

Fernando CALAMITA, Mounir BEN M'BAREK, Mirko DI VINCENZO & Mauro PELOROSSO

Dipartimento di Scienze della Terra,
Università di Chieti, Chieti Scalo, Italia

ABSTRACT

The study of the E-W sector of the Gran Sasso d'Italia salient (Figs. 1-18) allowed the reconstruction of the 3D geometry of the thrust planes, using the branch and cut-off line methodology (Fig. 19).
The following normal faults were identified: pre- and syn-orogenic faults, dislocated by the thrust planes and rotated inside the folds associated with the thrusting (Figs. 12-14); pre- and syn-orogenic faults reutilized during the Quaternary (Fig. 16); those with prevalently Quaternary activity (Fig. 17).
The correspondence between the Mesozoic palaeomargin architecture and the salient of the Gran Sasso thrust system testifies to the control exerted over the chain structure geometry by the preexistent discontinuities, which evolved in a context of inversion tectonics and with short-cut trajectories (Figs. 20-22). The paleomargin architecture also controlled the Messinian foredeep physiography, which is characterised by a structural high located at the carbonate platform, and by a depocenter sited above the pelagic basin immediately to the north of the carbonate platform. This structural high was partly inherited from the Oligocene-Miocene foreland evolution shown by the "Paleogene" discontinuity.
The Gran Sasso thrust system therefore came into being in a context of in-sequence propagation of the deformation, characterised by increasing SE-ward translation and a salient thrust plane geometry controlled by the preexistent discontinuities, which were connected with the Mesozoic palaeomargin evolution, the Oligocene-Miocene foreland and the Messinian foredeep. The reconstructed deformation context is compatible with vertical axis rotations, as evidenced by the palaeomagnetic data.

AIMS

The detailed geological mapping with macro- and mesostructural analyses carried out in three key sectors located along the E-W salient of the Gran Sasso d'Italia (Central Apennines) have allowed the following to be defined:
– the structural setting of the Apennine chain;
– the chronology of the normal fault systems and of their mode of interactions with the thrust planes;
– the control exerted by the Mesozoic paleomargin on Messinian foredeep physiography and on the geometry of the chain during its Pliocene evolution.

KEY WORDS

Mesozoic continental palaeomargin, Neogene orogenic system, fold and thrust belt, branch lines, cut-off lines, Central Apennines.

RIASSUNTO

Lo studio del settore E-W del saliente del Gran Sasso d'Italia (Figg. 1-18) ha consentito di ricostruire la geometria in 3D dei piani di sovrascorrimento rappresentata utilizzando il metodo delle branch-e cut-off lines (Fig. 19).
Sono state riconosciute faglie normali: pre- e sin-orogeniche, dislocate dai piani di sovrascorrimento e ruotate nell'ambito delle pieghe associate al thrusting (Figg. 12-14); pre- e sin-orogeniche riutilizzate durante il Quaternario (Fig. 16); a prevalente attività quaternaria (Fig. 17).
La corrispondenza tra l'architettura del paleomargine mesozoico e la geometria a saliente del sistema a thrust del Gran Sasso documenta il controllo esercitato dalle discontinuità pre-esistenti sulla geometria delle strutture della catena, evolute in un contesto d'inversione tettonica e con traiettoria di short-cut (Figg. 20-22).
L'architettura del paleomargine ha controllato anche la fisiografia dell'avanfossa messiniana caratterizzata da un alto strutturale localizzato in corrispondenza della piattaforma carbonatica e un depocentro ubicato al di sopra del bacino pelagico posto subito a nord della piattaforma stessa. Tale alto strutturale è in parte ereditato dall'evoluzione oligo-miocenica di avampaese documentata dalla lacuna paleogenica.
Pertanto, il sistema a thrust del Gran Sasso si è realizzato in un contesto di propagazione in sequenza della deformazione, caratterizzata da una entità di traslazione crescente verso SE e una geometria a saliente dei piani di sovrascorrimento controllata dalle discontinuità pre-esistenti, connesse all'evoluzione del paleomargine mesozoico, dell'avampaese oligo-miocenico e dell'avanfossa messiniana. Il contesto deformativo ricostruito è compatibile con le rotazioni su assi verticali evidenziate dai dati paleomagnetici.

GEOLOGICAL MAPS OF THE GRAN SASSO AREA

Legend — Structural and stratigraphic map

1) Syn and post-orogenic deposits unconformably overlying the pre-orogenic substratum

Continental deposits (*Quaternary*)

Conglomerati di Rigopiano (*Lower Pliocene*)

Conglomerati di Mt. Coppe (*Messinian? - Lower Pliocene*)

2) Syn-orogenic deposits (siliciclastic foredeep deposits)

Cellino Fm. (*Lower Pliocene*)

Laga Fm. Evaporitic and post-evaporitic Member, Vomano marls (*Messinian - Lower Pliocene*)

Laga Fm. Pre-evaporitic Member (*Messinian*)

3) Pre-orogenic substratum (carbonate succession)

Carbonate and shale deposits (*Miocene p.p.*)

Slope-basin carbonate succession (*Middle Lias - Oligocene*)

Carbonate platform succession (*Upper Triassic - Lower Lias*)

Persistent platform and margin carbonate succession (*Triassic - Malm*)

Thrust

Jurassic normal fault

Pre-thrusting normal fault a) reactivated during Quaternary

Normal fault with main activity during Quaternary

Normal fault

Fault

Tear fault

Anticline; a) pericline

Overturned anticline

Overturned syncline

1: Middle Pliocene - Upper Pleistocene post-orogenic deposits, unconformably overlying the fold-and-thrust belt in the periadriatic area; 2: Post-orogenic Plio-Quaternary deposits; 3: Lower Pliocene; 4: Messinian post-evaporitic-Lower Pliocene; 5: Messinian pre-evaporitic; 6: Upper Tortonian-Messinian pre-evaporitic; 7: Serravalian-Burdigalian; 8: Pre - orogenic substratum; 9: Allochthonous Molise Units 10: thrust; 11: anticline. **a**: Mt. Sibillini Unit; **b**: Laga Unit; **c**: Gran Sasso Unit.
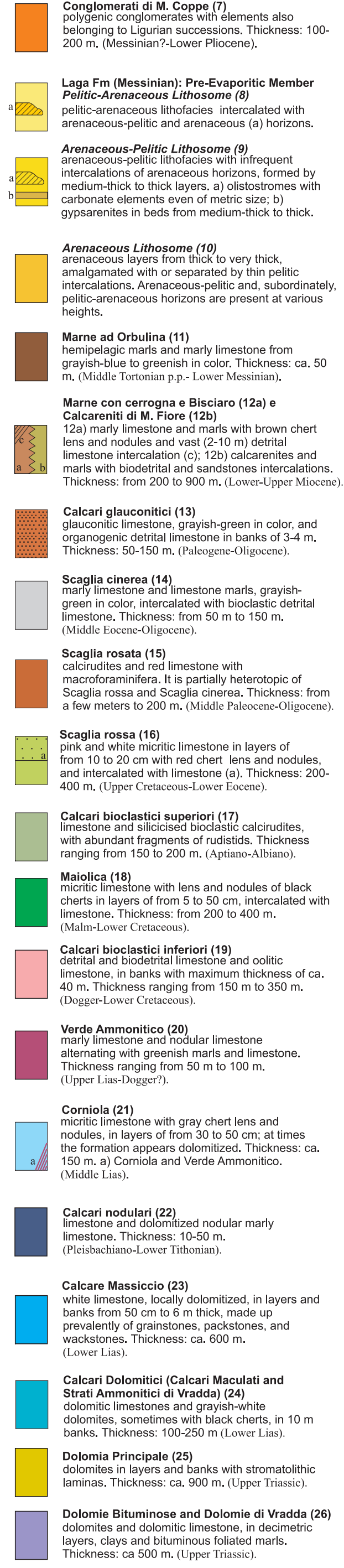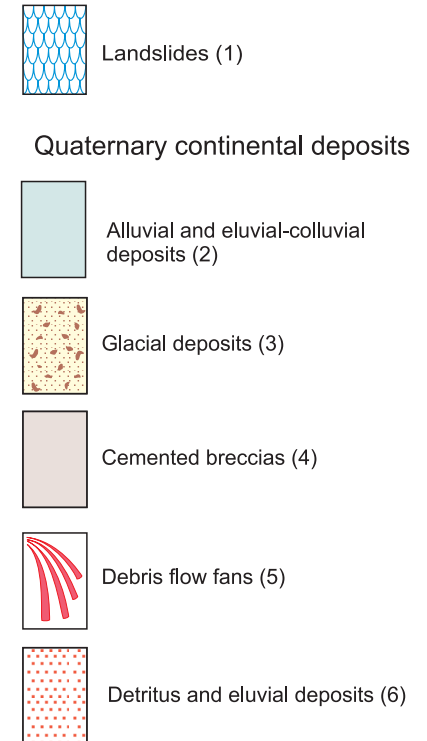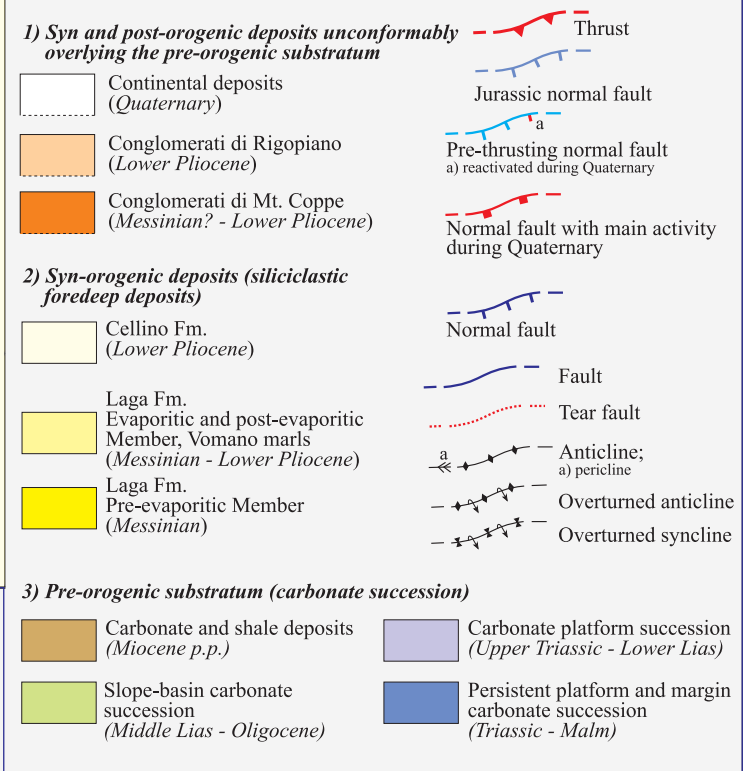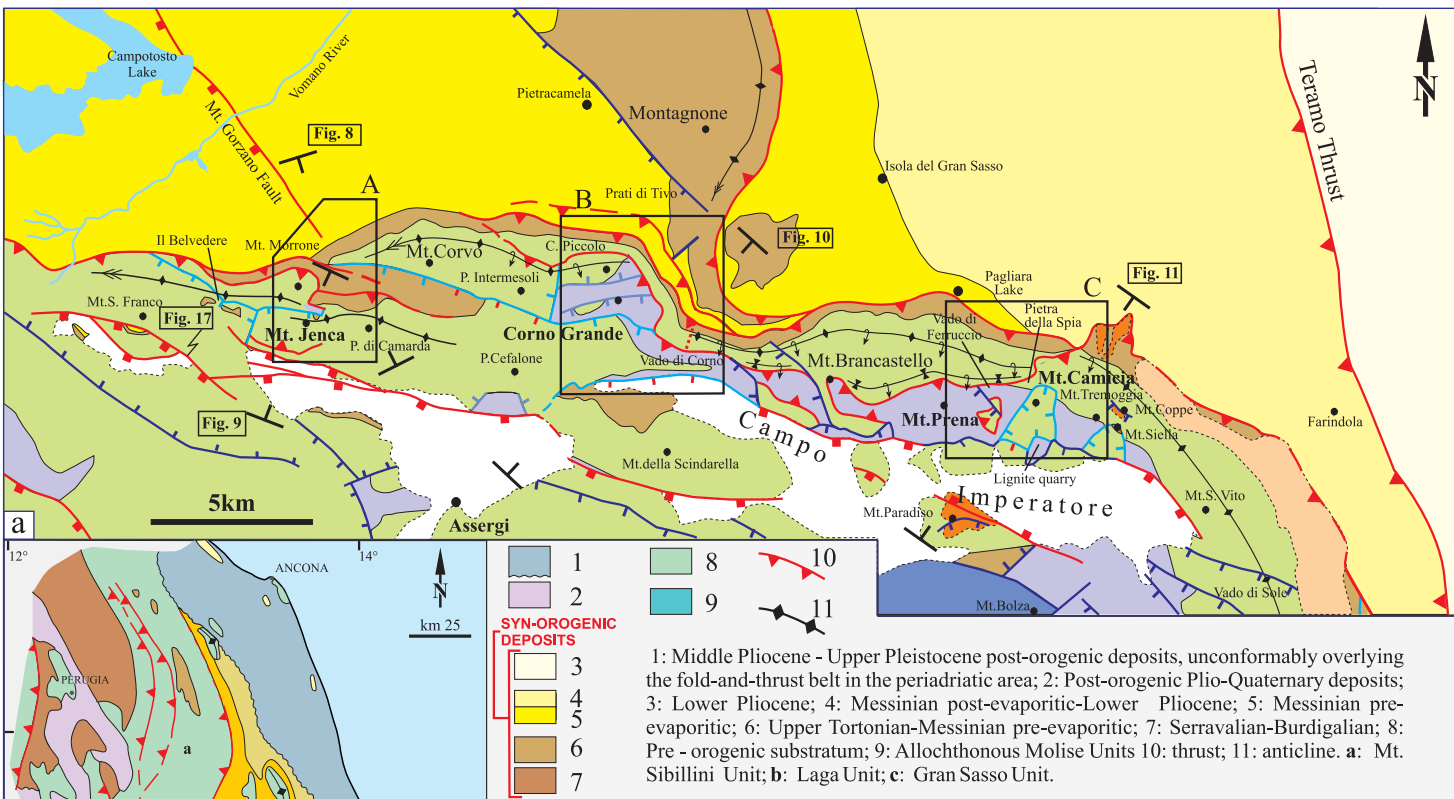
Fig. 1 - a) Structural sketch map of the Gran Sasso area; b) Tectonic sketch map of the Central Apennines of Italy. A, B and C are the geological map locations.

Legend — right column

Landslides (1)

Quaternary continental deposits

Alluvial and eluvial-colluvial deposits (2)

Glacial deposits (3)

Cemented breccias (4)

Debris flow fans (5)

Detritus and eluvial deposits (6)

Conglomerati di M. Coppe (7)
polygenic conglomerates with elements also belonging to Ligurian successions. Thickness: 100-200 m. (Messinian?-Lower Pliocene)

Laga Fm (Messinian): Pre-Evaporitic Member Pelitic-Arenaceous Lithosome (8)
pelitic-arenaceous lithofacies intercalated with arenaceous-pelitic and arenaceous (a) horizons.

Arenaceous-Pelitic Lithosome (9)
arenaceous-pelitic lithofacies with infrequent intercalations of arenaceous horizons, formed by medium-thick to thick layers. a) olistostromes with carbonate elements even of metric size; b) gypsarenites in beds from medium-thick to thick.

Arenaceous Lithosome (10)
arenaceous layers from thick to very thick, amalgamated with or separated by thin pelitic intercalations. Arenaceous-pelitic and, subordinately, pelitic-arenaceous horizons are present at various heights.

Marne ad Orbulina (11)
hemipelagic marls and marly limestone from grayish-blue to greenish in color. Thickness: ca. 50 m. (Middle Tortonian p.p.- Lower Messinian)

Marne con cerrogna e Bisciaro (12a) e Calcareniti di M. Fiore (12b)
12a) marly limestone and marls with brown chert lens and nodules and vast (2-10 m) detrital limestone intercalation (c); 12b) calcarenites and marls with biodetrital and sandstones intercalations. Thickness: from 200 to 900 m. (Lower-Upper Miocene)

Calcari glauconitici (13)
glauconitic limestone, grayish-green in color, and organogenic detrital limestone in banks of 3-4 m. Thickness: 50-150 m. (Paleogene-Oligocene)

Scaglia cinerea (14)
marly limestone and limestone marls, grayish-green in color, intercalated with bioclastic detrital limestone. Thickness: from 50 m to 150 m. (Middle Eocene-Oligocene)

Scaglia rosata (15)
calcirudites and red limestone with macroforaminifera. It is partially heterotopic of Scaglia rossa and Scaglia cinerea. Thickness: from a few meters to 200 m. (Middle Paleocene-Oligocene)

Scaglia rossa (16)
pink and white micritic limestone in layers of from 10 to 20 cm with red chert lens and nodules, and intercalated with limestone (a). Thickness: 200-400 m. (Upper Cretaceous-Lower Eocene)

Calcari bioclastici superiori (17)
limestone and silicicised bioclastic calcirudites, with abundant fragments of rudistids. Thickness ranging from 150 to 200 m. (Aptiano-Albiano)

Maiolica (18)
micritic limestone with lens and nodules of black cherts in layers of from 5 to 50 cm, intercalated with limestone. Thickness: from 200 to 400 m. (Malm-Lower Cretaceous)

Calcari bioclastici inferiori (19)
detrital and biodetrital limestone and oolitic limestone, in banks with maximum thickness of ca. 40 m. Thickness ranging from 150 m to 350 m. (Dogger-Lower Cretaceous)

Verde Ammonitico (20)
marly limestone and nodular limestone alternating with greenish marls and limestone. Thickness ranging from 50 m to 100 m. (Upper Lias-Dogger?)

Corniola (21)
micritic limestone with gray chert lens and nodules, in layers of from 30 to 50 cm; at times the formation appears dolomitized. Thickness: ca. 150 m. a) Corniola and Verde Ammonitico. (Middle Lias)

Calcari nodulari (22)
limestone and dolomitized nodular marly limestone. Thickness: 10-50 m. (Pleisbachiano-Lower Tithonian)

Calcare Massiccio (23)
white limestone, locally dolomitized, in layers and banks from 50 cm to 6 m thick, made up prevalently of grainstones, packstones, and wackestones. Thickness: ca. 600 m. (Lower Lias)

Calcari Dolomitici (Calcari Maculati e Strati Ammonitici di Vradda) (24)
dolomitic limestones and grayish-white dolomites, sometimes with black cherts, in 10 m banks. Thickness: 100-250 m (Lower Lias).

Dolomia Principale (25)
dolomites in layers and banks with stromatolithic laminas. Thickness: ca. 900 m. (Upper Triassic)

Dolomie Bituminose and Dolomie di Vradda (26)
dolomites and dolomitic limestone, in decimetric layers, clays and bituminous foliated marls. Thickness: ca 500 m. (Upper Triassic)
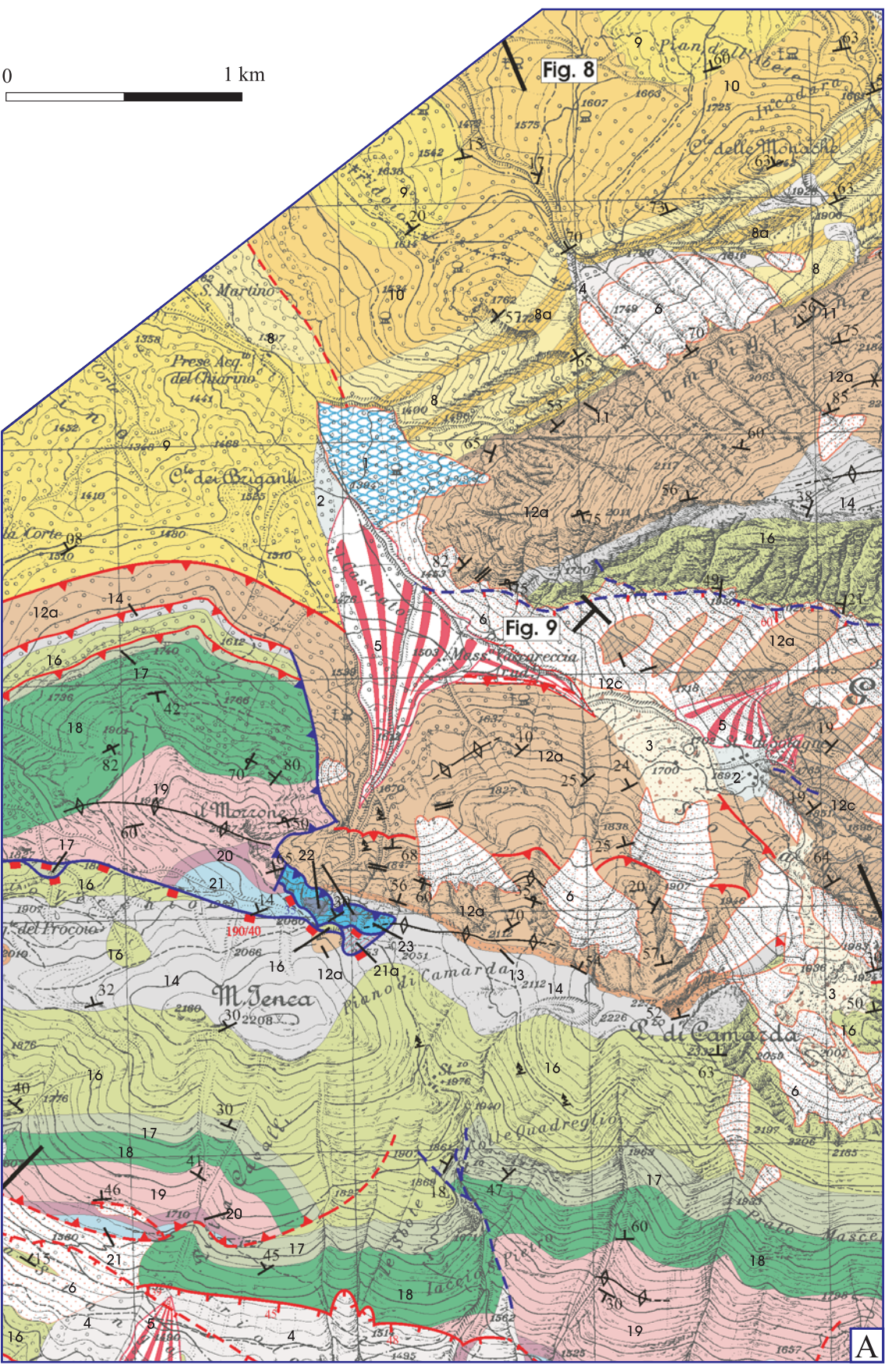
Fig. 1- A) Geological map; see Fig. 1a for location.

Fig. 1- B) Geological map; see Fig. 1a for location.

INTRODUCTION

The analysis of the role played by the preexistent discontinuities (normal faults connected with palaeomargin evolution and/or foreland bending of the chain itself) has been acquiring increasing importance in the study of the external portions of mountain chains. Indeed, detailed work carried out in external zones of the Appalachians, the Western Alps and the northern sector of the Pyrenees has led to an inversion tectonics context being evidenced; this includes reutilization of the preexistent normal faults as inverse motifs or their passive transport with a possible rotation inside the folds connected with the thrusts (BUTLER, 1989; WELBON, 1988; GILLCRIST et alii, 1989; McCLAY, 1989). The role played by the preexistent discontinuities on the thrust system geometry has been analysed also in the Apennines. Recent works have shown that the palaeomargin architecture exerted a clear control over the foredeep physiography and the 3D geometry of the chain structures that display a short-cut trajectory with respect to the pre- or syn-orogenic normal faults (BRUNI et alii, 1996; TAVARNELLI, 1996; SCISCIANI et alii, 2001; CALAMITA et alii, 2002) or an inversion sensu strictu (ARGNANI et alii, 1993; ARGNANI & GAMBERI, 1995; COWARD et alii, 1999).

METHODOLOGY

The investigations began with a detailed geological survey based on the identification of the Triassic-Pliocene stratigraphic units cropping out in the sectors examined and of the main tectonic discontinuities (Figs. 1A-C). The timing of the syn-sedimentary normal faults was reconstructed on the basis of facies and thickness variation and of the ages of the successions involved (Figs. 2 and 13-16).

The evaluation of the displacements and original features, and the reconstruction of pre-orogenic extensional fault system distribution were evidently modified by the extensive Quaternary reactivation and by the overprinting of the Pliocene compressional tectonics. These compressional elements (thrusts and folds) fragmented the Mesozoic and Cenozoic stratigraphic-structural pictures, which were dominated by rifting and foreland bending respectively.

This complex overlaying of deformational structures belonging to tectonic regimes of different significance and age can be explained by the restoration of geological sections along transects, across significant outcrops (Figs. 8-11).

The choice of the most significant key areas on which to perform detailed and combined macro- and meso-structural analyses logically derived from a direct knowledge of the study area, which allowed the basic geologic mapping to be carried out. The stratigraphy, tectonics and kinematics of the individual key areas constrained the two-dimensional restoration (Fig. 11a).

The main objective of this operation is to understand the meaning of the numerous faults present, to assess their displacement, to determine their relationship and to establish the age of their activation and/or reactivation.

In particular, the 3D geometry of the thrust planes was reconstructed using branch and cut-off line methodology (BOYER & ELLIOT, 1982; HOSSACK, 1983).

The branch lines are where the thrusts branch together. Thrust sheets will have a limited spatial extent and be surrounded by branch lines with segments that are eroded and buried (Fig. 19a).

The cut-off lines represent the intersection between the thrust plane and the stratigraphic markers.

These lines mimic the ramps, and the hangingwall and footwall cut-off lines should be parallel to each other. Their distance on the map allowed the evaluation of the horizontal component of the thrust displacement parallel to the direction of the tectonic transport (Fig. 19b). The classical criteria of structural geology and stratigraphy were adopted to study the normal faults. The geometric analysis allowed a definition of the fault plane dip-angle, its cut-off angle with respect to the bedding and the dip of the bedding in the respective hangingwalls and footwalls of the fault (Fig. 12).

The kinematic analysis allowed the identification of the relative movement of the blocks, both with regard to the main plane and to the synthetic planes associated with it. Mechanical striae were considered (Figs. 12 and 17), as well as possible fabrics, in particular characterising the fault rocks associated with the thrust planes (Fig. 7). Relative and absolute dating of the faults was carried out. The absolute dating is constrained by the ages of the most recent deposits involved and of the ancient ones not involved, by the age of the formations displaying lateral variations in thickness and
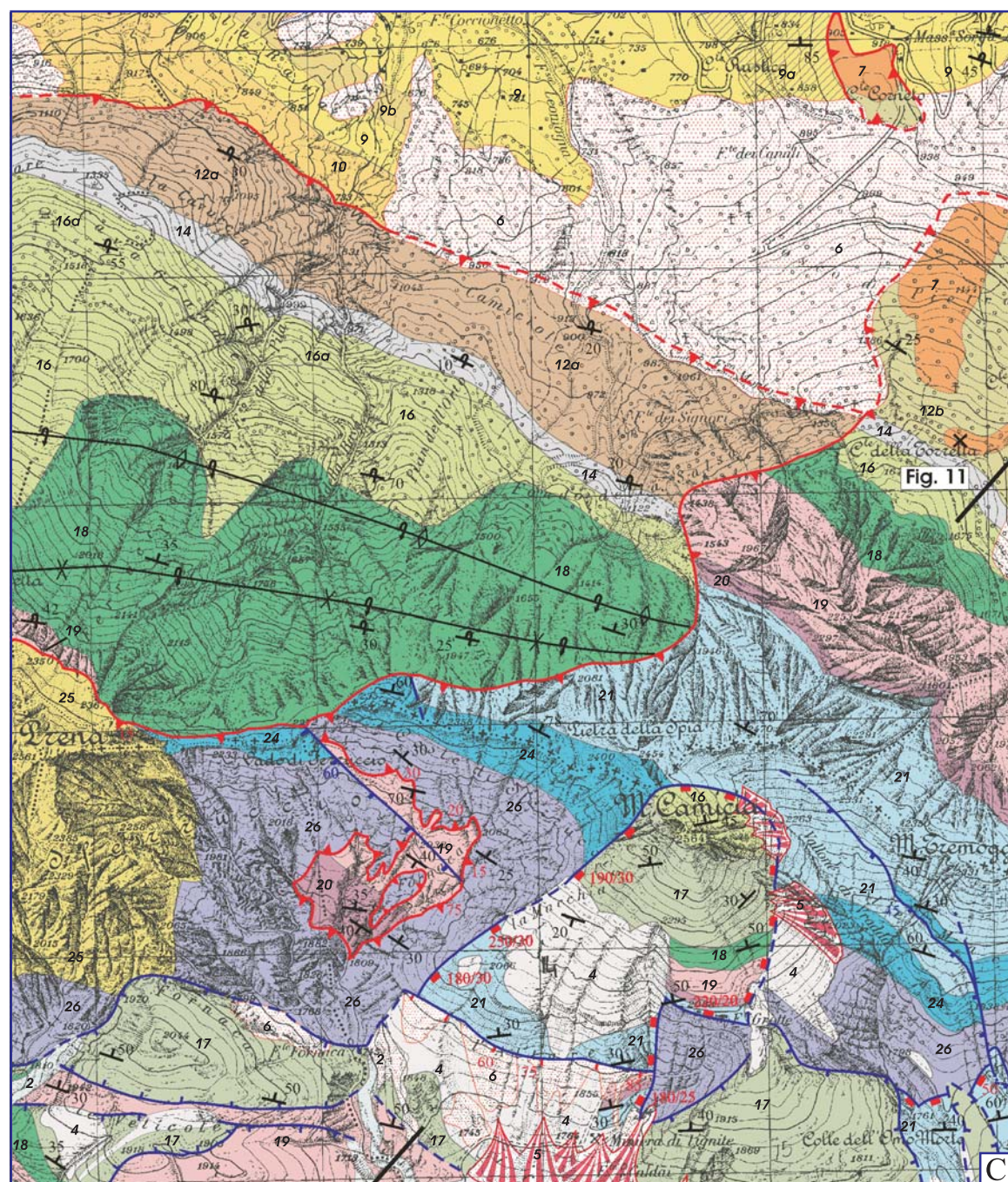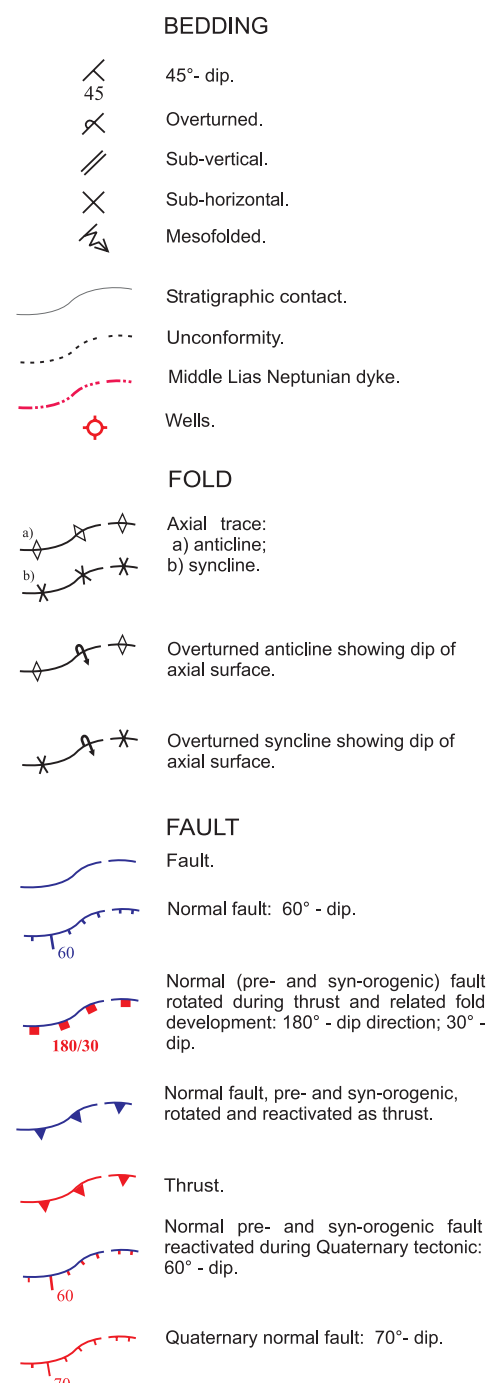

BEDDING

- 45°- dip.
- Overturned.
- Sub-vertical.
- Sub-horizontal.
- Mesofolded.

- Stratigraphic contact.
- Unconformity.
- Middle Lias Neptunian dyke.
- Wells.

FOLD

- Axial trace:
  a) anticline;
  b) syncline.
- Overturned anticline showing dip of axial surface.
- Overturned syncline showing dip of axial surface.

FAULT

- Fault.
- Normal fault: 60° - dip.
- Normal (pre- and syn-orogenic) fault rotated during thrust and related fold development: 180° - dip direction; 30° - dip.
- Normal fault, pre- and syn-orogenic, rotated and reactivated as thrust.
- Thrust.
- Normal pre- and syn-orogenic fault reactivated during Quaternary tectonic: 60° - dip.
- Quaternary normal fault: 70°- dip.
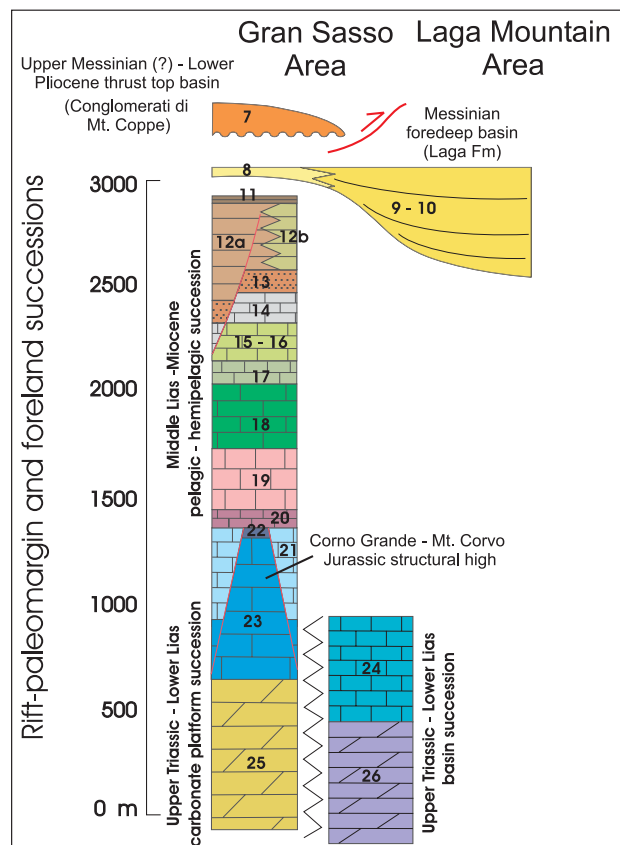
Fig. 1C - Geological map; see Fig. 1a for location.

Fig. 2 - *Stratigraphic section of the Gran Sasso and Laga Mountain Area. The thickness of the thrust top and foredeep basins are not in scale.*
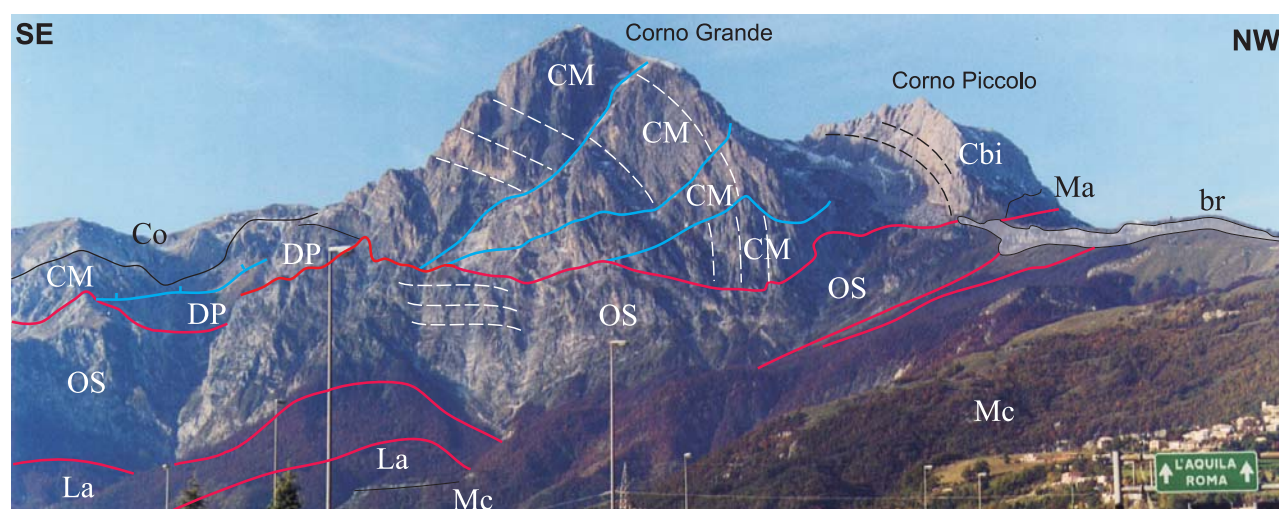
facies between the hangingwall and the footwall, as well as by the presence of megabreccias associated with the palaeoscarps, which are controlled by the fault activity, and by neptunean dykes (Figs. 2 and 13-16).

The Quaternary activity of the normal faults, well documented by the presence of fault scarps (Fig. 17) where dislocated continental Quaternary deposits can often be observed, was defined by means of the amount of geomorphologic displacement calculated on the basis of the displacement of plane-surface remnants, as proposed by COLTORTI & PIERUCCINI (2000) and PIZZI *et alii* (2002). This criterion thus allowed identification of the faults that exclusively showed Quaternary activity, in which geological displacement is equal to geomorphologic displacement, whereas the faults that were reutilized in the Quaternary show higher geological than geomorphologic displacement.

The relative chronology was established on the basis of cross-cut relationships (Figs. 1A-C and 6), kinematic and deformational compatibility, and the compatibility of the structures with vertical axis rotation as revealed by palaeomagnetism. Moreover, the restoration of

the geological sections allowed the reconstructed chronological relationships to be further constrained (Fig. 11a). Finally, the Messinian foredeep physiography was reconstructed using the variations in thickness and in facies of siliciclastic deposits; this allowed the geometry and bending mechanisms, as well as their relationship with the Mesozoic palaeomargin architecture (Figs. 20-22), to be evidenced and/or hypothesized for the foreland.

GEOLOGICAL SETTING

The Gran Sasso thrust forms a spectacular salient structure of the central external Apennines (GHISETTI & VEZZANI, 1990; 1991). It juxtaposes the carbonate tectonic unit, which is involved in folds with axial trends parallel to that of the thrust plane, on the Laga tectonic Unit, characterised by N-S-trending folds and thrusts (Figs. 1a and 1b). The Gran Sasso tectonic unit consists of Triassic-Miocene successions of the Latium-Abruzzi carbonate platform and of its transition zone into the Marchean pelagic basin, and of Messinian foredeep siliciclastic deposits (Laga Fm.). Unconformably on the chain elements lie the Conglomerati di Mt. Coppe (Fig. 2) (Messinian-Lower Pliocene) and Conglomerati di Rigopiano (Lower Pliocene) piggy-back basins (ADAMOLI *et alii*, 1978; GHISETTI *et alii*, 1990; BIGOZZI *et alii*, 1991; CENTAMORE *et alii*, 1991; VAN KONIJNENBURG *et alii*, 1999).

TECTONIC AND KINEMATIC EVOLUTION

The essential features of the Gran Sasso thrust have been known for some time as described in literature (BALLY, 1954; GHISETTI & VEZZANI, 1986). The study carried out (geological survey and structural analyses) allowed us to evidence the relationship between the two thrust planes that reveal a tectonic lens located between the hangingwall (Gran Sasso tectonic Unit) and the footwall (Laga tectonic Unit) (Fig. 19a). The

Fig. 3 - *Panoramic view of the E-W trending Gran Sasso thrust front. DP: Dolomia Principale; CM: Calcare Massiccio; Cbi: Calcari bioclastici inferiori; Ma: Maiolica; OS: Jurassic-Miocene overturned succession; Mc: Marne con cerrogna; La: Laga Fm.; br: Quaternary cemented breccias; dashed line: bedding; red line: thrust; blue line: normal fault. (Fig. 1B).*

Fig. 4 - *Upper thrust along which the Dolomia Principale (DP) is juxtaposed onto the pelagic sequence belonging to the intermediate Unit (Cbi: Calcari bioclastici inferiori; Ma: Maiolica). The footwall block is involved in an overturned syncline trending more or less E-W. (Fig. 1C).*
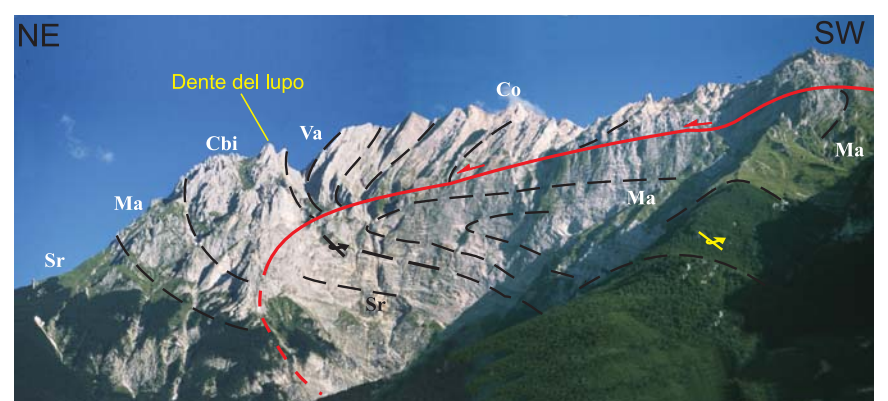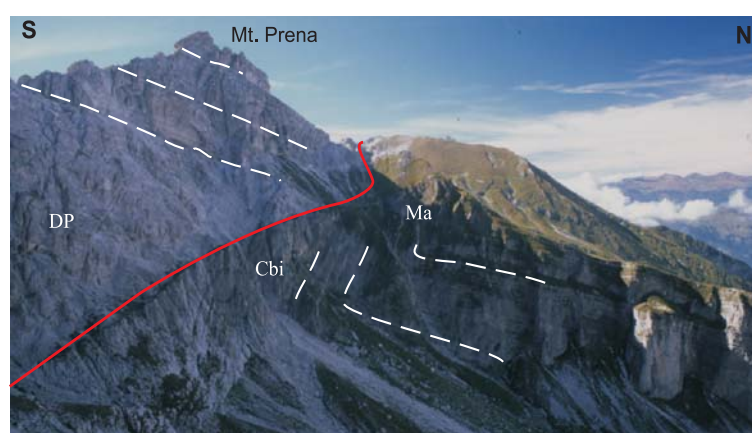
Fig. 5 - *Panoramic view of the antiformal folded Upper thrust. The footwall block, corresponding to the Middle Unit, is deformed by recumbent folds. Co: Corniola; Va: Verde Ammonitico; Cbi: Calcari bioclastici inferiori; Ma: Maiolica; Sr: Scaglia Rossa. (Fig. 1C).*

Fig. 6 - *Panoramic view of the tectonic window of Fornaca. DB: Dolomie Bituminose; DP: Dolomia Principale (DP: heteropic of Dolomie Bituminose); CD: Calcari Dolomitici; Va-Cbi: Verde Ammonitico-Calcari bioclastici inferiori.*

upper thrust plane crops out continuously along the whole central eastern section of the Gran Sasso (Figs. 1B-C and 3-6); it is folded in antiform and branches eastward with the lower thrust in the leading branch line (Fig. 1C).

The geological-structural features of the upper thrust plane can be observed in the Fornaca tectonic window where the hangingwall, consisting of Dolomie Bituminose, the tectonic lens (Verde Ammonitico and Calcari bioclastici inferiori), and the thrust plane (Fig. 6) crop out. This dips SSW (200°-220°) with a dip angle of 20°-30° and has striae pitching 70°W, showing inverse kinematics with a left-lateral component. A shear zone of metric thickness is present, characterised by a planar fabric defined by pervasive shear planes and cataclastic flux bands in the Dolomie Bituminose marly lithology (Fig. 7). This fabric separates centimetric-sized lithons, iso-oriented by cataclastic flux (the foliated cataclasites of GHISETTI & VEZZANI, 1986), and lies parallel to the thrust plane. A normal fault with decametric-sized displacement and dipping SSW (220°), with a dip angle of 60°-80°, dislocates the thrust plane, and is therefore subsequent to it in time (Figs. 1C and 6).

The lower thrust plane overlays the carbonate units on the Laga Fm. siliciclastic deposits. Westward, the two thrust planes progressively lose their amount of displacement, assuming the characteristic of blind thrusts, and have an en-échelon relationship with the Mt. Jenca - Mt. S. Franco thrusts (Figs. 1a and 8-11). In fact, at Mt. Corvo, the stratigraphic transition can be observed between the carbonate sequence and the Laga siliciclastic deposits (Fig. 16).

SSW-dipping normal faults with a maximum displacement of about 2500 m characterise this sector of the Apennine chain (Fig. 1). On the basis of their relative and absolute chronology, the following were recognised:

• Pre- and syn-orogenic faults rotated to a low dip angle (the Mt. Camicia and Mt. Jenca faults, Figs. 12 and 13) or an opposite dip-direction and an apparently inverse aspect (the Corno Grande "Passo del Cannone" fault, Fig. 14). To the south, the Mt. Jenca fault delimits a structural high, which is characterised by the Mt. Jenca-Mt. S. Franco condensed Jurassic succession. This was reutilized during the Miocene and rotated in the southern limb of the anticline. The conjugated fault that to the north bordered the same Jurassic high was also involved in the rotation; it inverted its dip direction and took on an inverse aspect. The presence of mesofolds (Fig. 13) suggests its reutilization as a thrust. Pre-orogenic (Mesozoic) activity can be found for the Passo del Cannone fault; this is suggested by the presence of the condensed

Fig. 7 - *Shear zone related to the upper thrust plane cropping out at the Fornaca tectonic window and involving the Dolomie Bituminose Formation. It is characterized by a pervasive shear plane and centimetric-sized lithones (planar fabric), parallel to the thrust plane* (T). (a) *Close-up showing the planar fabric. The stereonet shows the geometry and kinematics of the thrust.*
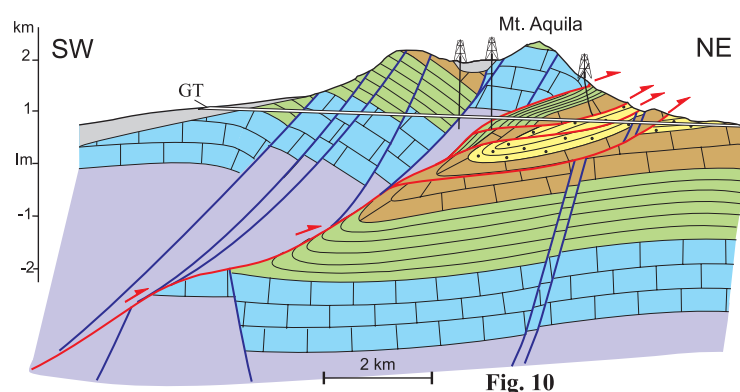

Legend:

- Continental deposits (*Quaternary*)
- Conglomerati di Mt. Coppe (*Messinian? - Lower Pliocene*)
- Laga Fm. (*Messinian*)
- Emipelagic succession (*Lower Miocene - Messinian*)
- Pelagic succession (*Middle Lias - Oligocene*)
- Calcare Massiccio Fm. (Figs. 8-10) or Calcari Dolomitici (Figs. 11 and 11a) (*Upper Triassic - Lower Lias*)
- Dolomie Bituminose and Dolomie di Vradda Fms. (Figs. 11 and 11a) or Dolomia Principale Fm. (Fig. 10) (*Upper Triassic*) and Basement (?)
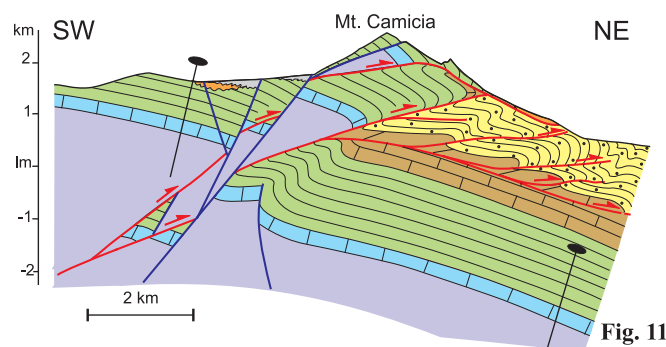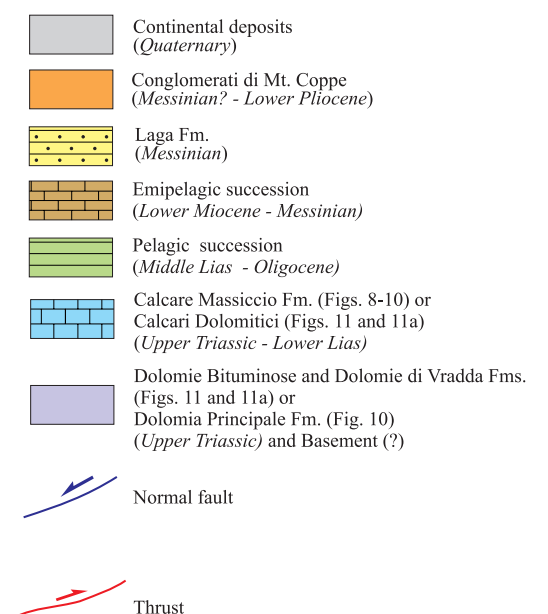- Normal fault
- Thrust

Schematic cross-sections across the E-W-trending Gran Sasso thrust system

Fig. 8: *Mt. Corvo cross-section;*
Fig. 9: *Mt. Jenca cross-section;*
Fig.10: *Corno Grande cross-section (Gran Sasso tunnel: GT);*
Fig. 11: *Mt. Camicia cross-section;*
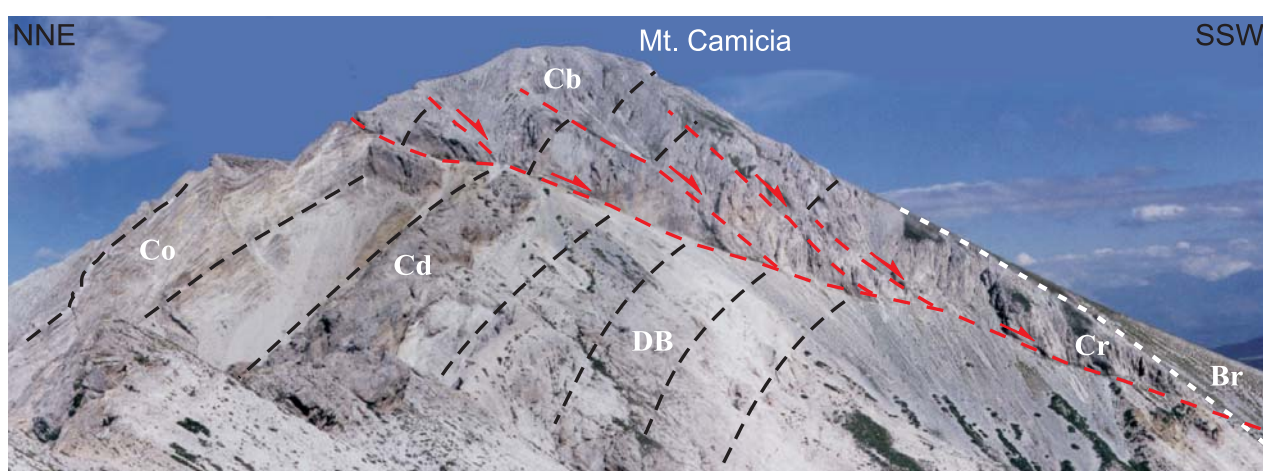Fig. 11a: *Mt. Camicia restored cross-section.*

Fig. 12 - *The Mt. Camicia low-angle normal fault and relative synthetic fault planes (Inset C).* DB: *Dolomie Bituminose (Upper Triassic);* Cd: *Calcari Dolomitici (Lower Lias);* Co: *Corniola (Middle Lias);* Cbs: *Calcari bioclastici superiori (Lower Cretaceous);* Cb: *bioclastic Calcarenites (Cretaceous-Oligocene);* Br: *continental deposits (Quaternary); C-a: Cut-off angle. The stereonet shows the geometry and kinematics of the fault.*

succession in the footwall (Corno Grande) and the complete one in the hangingwall (Corno Piccolo). The rotation occurred during the development of the Corno Grande-Mt. Corvo anticline (Fig. 8);

• Pre- and syn-orogenic faults reutilized during the extensional tectonics in the Quaternary (the Mt. Corvo - Corno Grande "Tre Stelle" fault, Fig. 16). The pre-orogenic activity of this structure is evidenced in the sector near the Corno Grande (Fig. 1B) by the presence of complete Jurassic successions in the hangingwall (Mt. Aquila) and condensed successions in the footwall (Corno Grande).

In the latter sector, Jurassic and Cretaceous neptunian dykes are present, associated with the above-mentioned extensional tectonics (Fig. 15). The syn-orogenic activity of the structure connected with foreland flexural processes during the Miocene is suggested by variations in the facies and the thickness of the Miocene deposits (Marne con cerrogna) between the hangingwall and footwall (Fig. 16).

Its reutilization during the Quaternary is documented by the presence of fault scarps near the Val Maone and by palaeoseismological evidence (GIRAUDI & FREZZOTTI, 1995; ADAMOLI *et alii*, 2003);

• Faults with prevalently Quaternary activity (Fig. 17). These structures form the Assergi and Campo Imperatore systems, comprising en-échelon faults that border the intra-mountain basins. In particular, in the Assergi system, a displacement of about 1000 m, analogous to the geomorphological displacement, can be seen (Figs. 9 and 10). Fault scarps, along which Quaternary continental deposits are also found, are associated with them.

Fig. 13 - *The Mt. Jenca Jurassic structural high characterized by a reduced sequence (CM: Calcare Massiccio; Cn: Calcari Nodulari). The fault-bounded high was reactivated during the foreland syn-orogenic flexure and was rotated within the forelimb of the Mt. Jenca anticline. A″-A‴ undeformed stage. Co: Corniola; Va: Verde Ammonitico; Sc: Scaglia cinerea; Mc: Marne con cerrogna. (Figs. 1A and 9).*

STRUCTURAL EVOLUTION OF THE GRAN SASSO AREA

The geological mapping and macro- and meso-structural analyses of the E-W trending sector of the Gran Sasso d'Italia salient allowed us to evidence the tectonic features of this portion of the Pliocene Apennine chain, which is characterised by interactions between the normal fault systems and the thrust planes, as well as its kinematics (Figs. 1-18). The analogy between the palaeomargin trend of the Latium-Abruzzi platform and the Gran Sasso salient (an arcuated trend of the thrust planes and associate folds, Figs. 20 and 21) shows the control exerted by the Mesozoic palaeomargin over the geometry of the structures of the chain.

In particular, by applying the methodologies described, the following can be reconstructed:

• The geological and structural setting of this sector of the Apennine chain (Figs. 1-2, 8-11, 18 and 19);

• The chronological relationships between the normal faults and thrust planes (Figs. 1A-C, 6 and 16-21);

• The main deformational events (Figs. 21 and 22).

The structural and morphological elevation of this sector of the Apennine chain creates spectacular outcrop conditions that enable the proposed investigative methodology to be applied (Figs. 3-6 and 12).

The structural setting of this portion of the chain is defined by two main WNW-ESE thrust planes with a ca 30° southward dip angle. To the west, they show tip points in the neighbourhood of Mt. Corvo, whereas the amount of displacement increases progressively towards the east (Figs. 1a and A).

North of Mt. Camicia, the upper thrust is folded in antiforms and joins up with the lower thrust along the leading branch line that limits the
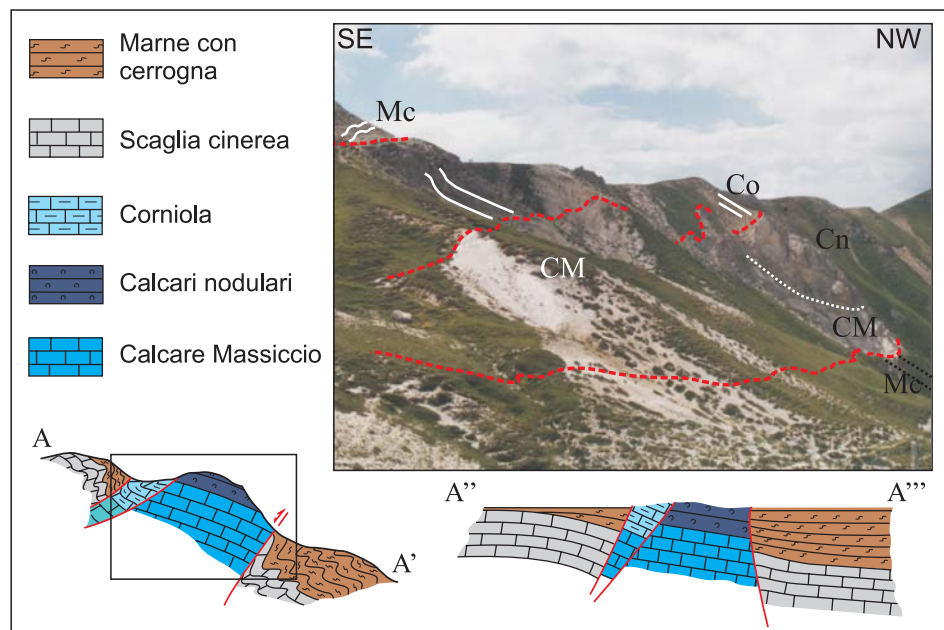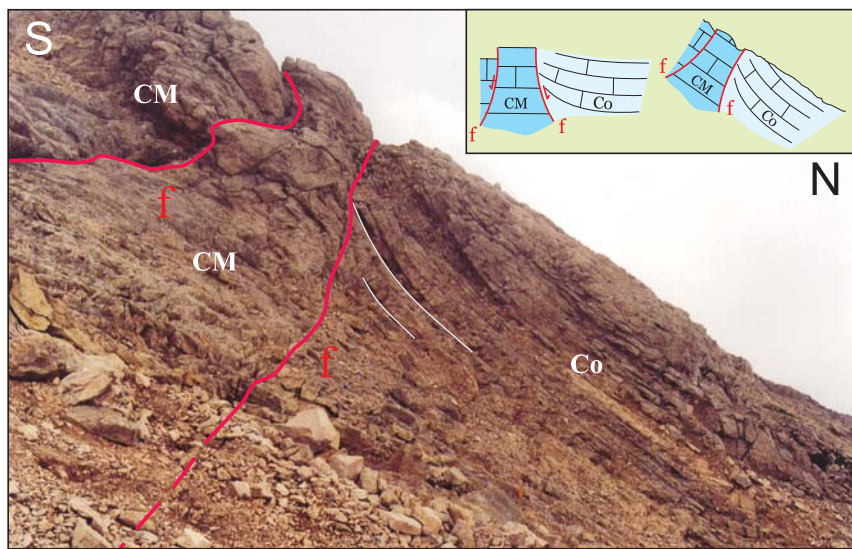

Fig. 14 - *Overturned Jurassic fault (f) in the Corno Grande area, rotated within the forelimb of the Corno Grande-Mt. Corvo anticline. CM: Calcare Massiccio; Co: Corniola. (Inset B). a) undeformed stage; b) present-day stage.*
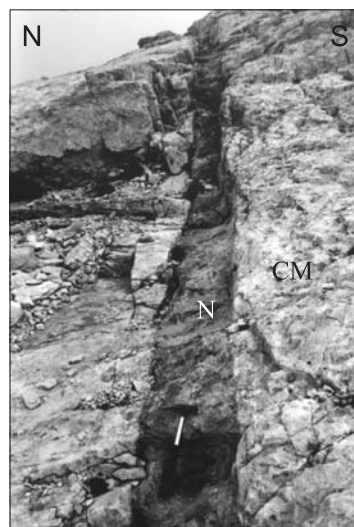

Fig. 15 - *Middle Lias neptunian dykes (N), trending E-W, in the Calcare Massiccio Fm. "CM" (Corno Grande).*

Fig. 16 - *Panoramic view of Mt. Corvo showing: a) the Mt. Corvo - Tre Selle normal fault (TS) that realises the contact between the Marne con cerrogna (Mc-Mcd: coarse grained levels) and the Scaglia rossa (Sr), the Scaglia cinerea (Sc) and the Bisciaro (Bs); b) the near vertical northern limb of the Mt. Corvo anticline where the Oligo-Miocene succession, the Marne a Pteropodi (Mp) and the Laga Fm. (La) crop out. (Fig. 1A).*

Fig. 17- *Quaternary normal fault which displaces the upper Pleistocene continental deposits in the Assergi intra-mountain basin. La: Laga Fm. Ma: Maiolica (Fig. 1a). The stereonet shows the geometry and kinematics of the fault. The red arrows evidence the fault scarps.*
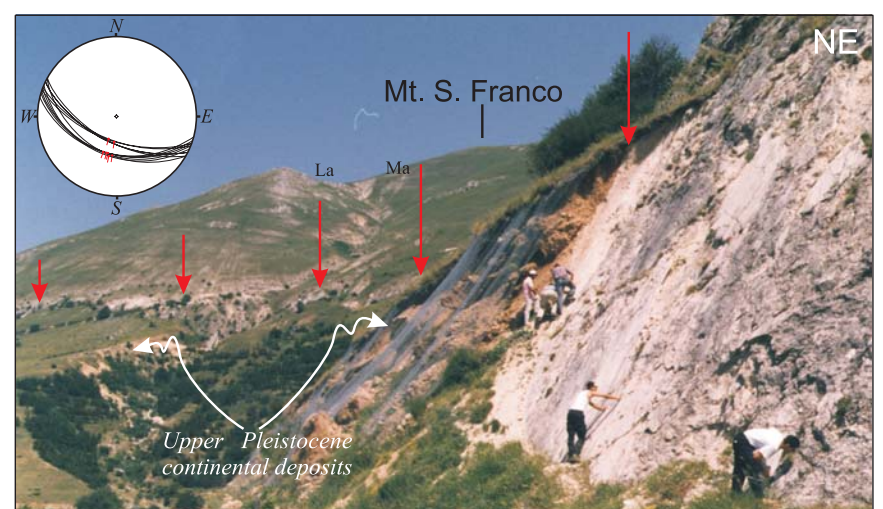
tectonic interposed lens (Figs. 5 and 19a). The foliated cataclasites associated with the thrust plane show left-lateral, transpressive kinematics of the structure (Fig. 7).

On the basis of the normal faults chronology and of their relationships with the thrust planes, the following normal fault systems were recognized: pre- and syn-orogenic faults dislocated by the thrust planes and rotated inside the folds associated with the thrusting (Figs. 12-14); pre- and syn-orogenic faults reutilized during the Quaternary (Fig. 16); faults of prevalently Quaternary activity (Fig. 17).

The evaluation of the data sets obtained in the field and restoration of the geological sections allowed us to define the following deformational events (Fig. 22):

1) **Triassic-Jurassic extensional tectonics** (rifting and development of passive margins). This event was reconstructed from the presence of normal faults that identify structural highs and lows with condensed and continuous sedimentation respectively. The most evident example of this is the Corno Grande structural high, delimited by the Tre Stelle fault to the south and the Passo del Cannone fault to the north (Figs. 2, 13 and 14);

2) **foreland tectonics** characterised by the reutilization of the previous normal faults and evidenced by variations in thickness and in facies inside the Cretaceous-Miocene successions (Figs. 13 and 16);

3) **Messinian foredeep bending** with the development of an articulated physiography controlled by the palaeomargin and foreland architecture (Figs. 2 and 20);

4) **Pliocene thrusting** with the development of the Gran Sasso salient and the Mt. Coppe and Rigopiano thrust-top basins (Figs. 2-7);

5) **Quaternary normal faults** that reutilized the preexistent discontinuity and generated the intra-Apennine depressions of Campo Imperatore and Assergi (Figs. 17 and 18).

Observing the analogy between the paleomargin trend of the Latium-Abruzzi carbonate platform and the Gran Sasso salient, the control exerted by the Mesozoic palaeomargin over the geometry of the thrusts and the related folds appears evident (Figs. 1a, 1b and 21). The palaeomargin architecture has also controlled the physiography of the Messinian foredeep, that presents a depocenter located in the Marchean palaeobasin and a high corresponding to the Latium-Abruzzi carbonate platform (Fig. 20). This high may be partly inherited from the foreland deformation, testified by the Paleogene
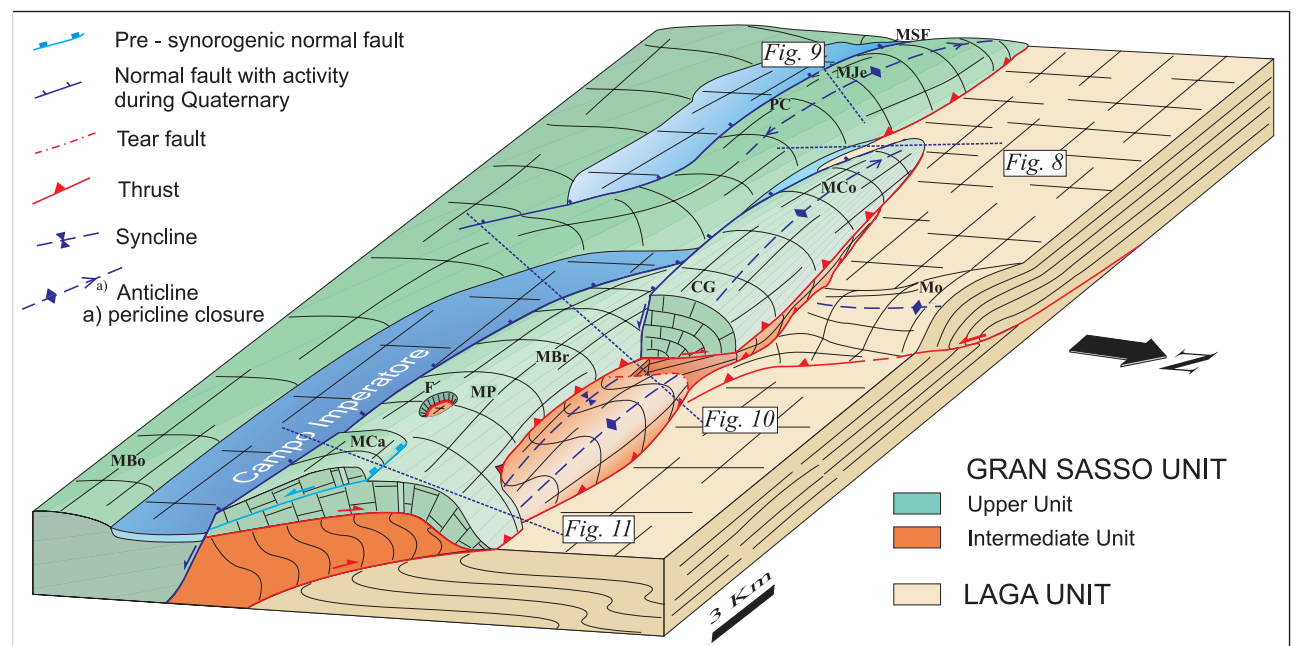
discontinuity that can be observed in the Latium-Abruzzi carbonate platform (Fig. 21).

In conclusion, a precise series of field investigations constrain our proposed interpretation: the Gran Sasso salient came into being during the Upper Messinian-Middle Pliocene, in a context of in-sequence propagation of the deformation, as testified by the folding of the upper thrust as a result of the development of the lower thrust and of the relative hangingwall anticline (Figs. 5 and 11). This is characterised SE-ward by an increasing amount of translation (a discordant trend with respect to the footwall structures "the Laga tectonic Unit") controlled by the preexistent discontinuities (Figs. 8-11). The foreland structural association is characterised by WNW-ESE-trending normal faults and by transcurrent-transpressive motifs trending N-S and E-W, controlled by Mesozoic palaeomargin

discontinuities, rotated and reutilized as thrust planes during the development of the chain (CALAMITA et alii, 2003 and references therein). The reconstructed deformational context (Fig. 22), both in terms of structuring of the chain and of foreland deformation, is compatible with the vertical axis rotation evidenced by the palaeomagnetic data analysed by DE LA PIERRE et alii (1992) and SPERANZA et alii (2001).

Fig. 18 - *Block diagram of the E-W-trending Gran Sasso thrust front from Mt. Camicia to Mt. S. Franco. Mbo: Mt. Bolza; MCa: Mt. Camicia; MP: Mt. Prena; F: Fornaca tectonic window; MBr: Mt. Brancastello; CG: Corno Grande; Mo: Montagnone; MCo: Mt. Corvo; PC: Pizzo di Camarda; MJe: Mt. Jenca; MSF: Mt. S. Franco.*
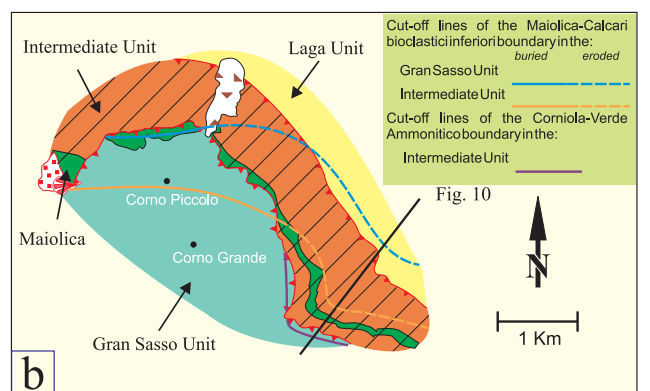

Fig. 19 - *Structural sketch map of the Gran Sasso area showing the branch-line pattern of the Gran Sasso thrust system (a) and the cut-off line distribution at the Corno Grande-Corno Piccolo area (b).*
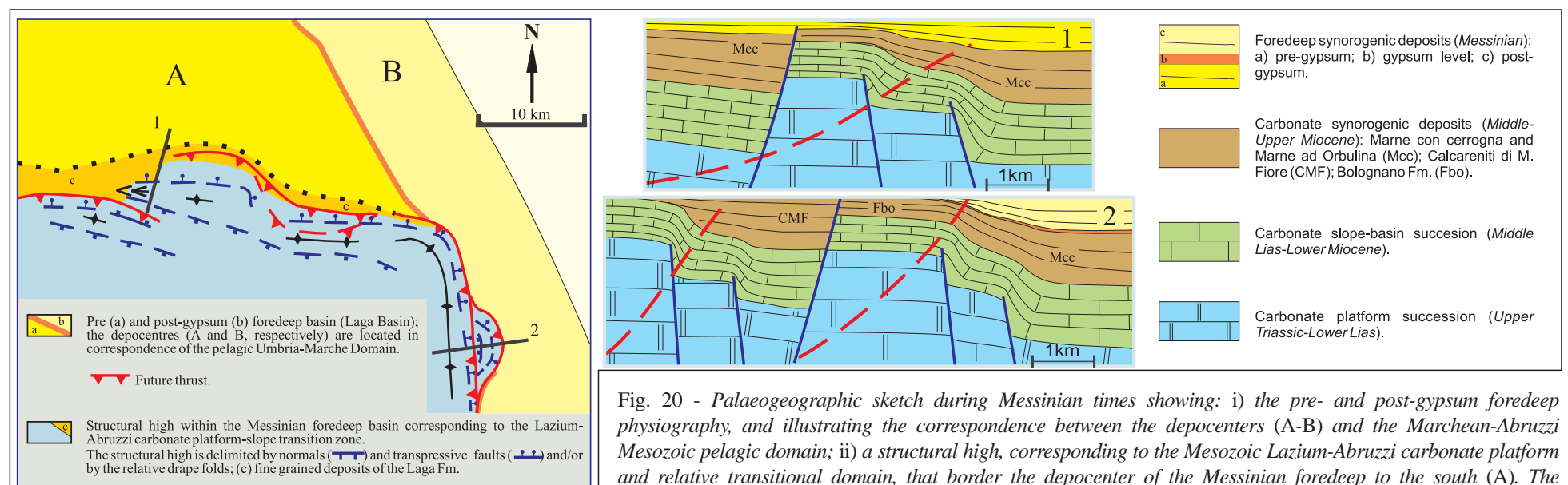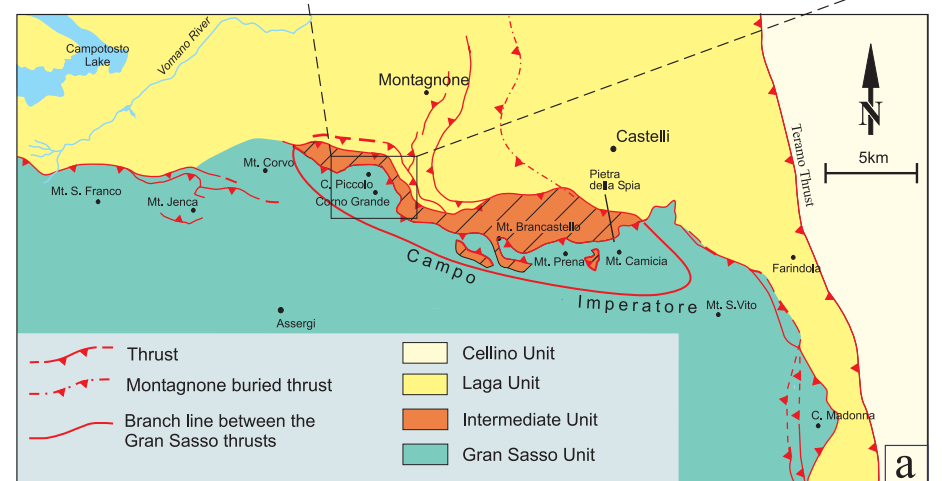

Fig. 20 - *Palaeogeographic sketch during Messinian times showing: i) the pre- and post-gypsum foredeep physiography, and illustrating the correspondence between the depocenters (A-B) and the Marchean-Abruzzi Mesozoic pelagic domain; ii) a structural high, corresponding to the Mesozoic Lazium-Abruzzi carbonate platform and relative transitional domain, that border the depocenter of the Messinian foredeep to the south (A). The palaeomargin architecture and the foredeep physiography control the thrust ramp location and their geometry.*
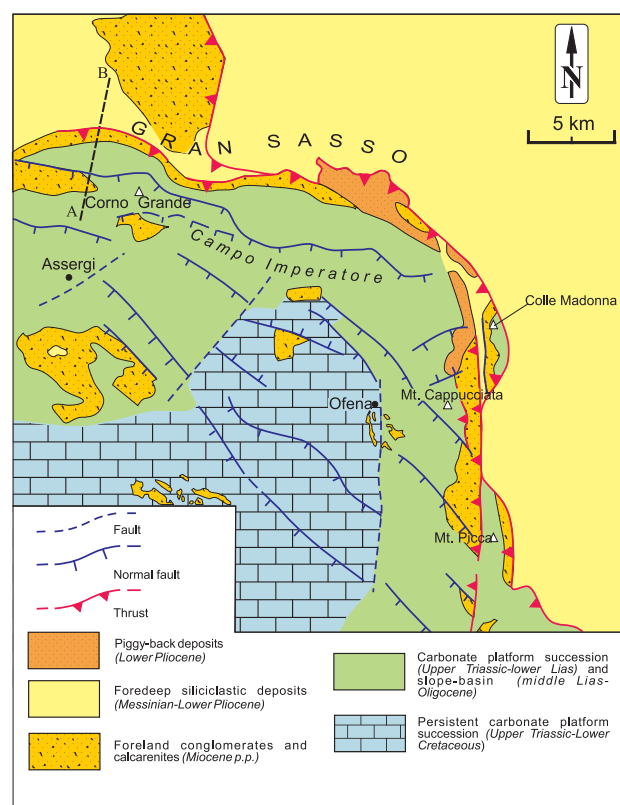
Fig. 21 - *Structural sketch showing the analogy between the paleomargin trend of the Latium-Abruzzi carbonate platform and the Gran Sasso salient geometry. The A-B section refers to Fig. 22.*

Fig. 22 - *Sketches showing the main Triassic-Quaternary deformation steps of the study area.*

REFERENCES

ADAMOLI L., BERTINI T., CHIOCCHINI M., DEIANA G., MANCINELLI A., PIERUCCINI U. & ROMANO A. (1978) - *Ricerche geologiche sul Mesozoico del Gran Sasso d'Italia (Abruzzo). II. Evoluzione tettonico-sedimentaria dal Trias superiore al Cretacico inferiore dell'area compresa tra il Corno Grande e S. Stefano Sessanio (F° 140 Teramo).* Studi Geol. Camerti (1981-82), **VII**: 7-17.

ADAMOLI L., CALAMITA F. & PELOROSSO M. (2003) - *Gran Sasso d'Italia: dai Prati di Tivo ai Prati di Tivo attraverso il Ghiacciaio del Calderone, il Corno Grande, Campo Pericoli e la Val Maone.* A cura della Soc. Geol. It. BE.MA, 102-112.

ARGNANI A. & GAMBERI F. (1995) - *Stili strutturali al fronte della catena appenninica nell'Adriatico centrosettentrionale.* Studi Geol. Camerti, Vol. Spec. (1995/**1**): 19-28.

ARGNANI A., FAVALI P., FRUGONI F., GASPERI M., LIGI M., MARANI M.M., MATTIETTI G. & MELE G. (1993) - *Foreland deformation patterns in Southern Adriatic sea.* Ann. Geofis., **36**(2): 229-247.

BALLY A.W. (1954) - *Geologische Untersuchungen.* In: den SE Abruzzen. Zurich, Buhler Buchdruck, 289 pp.

BIGOZZI A., CIARAPICA G., CIRILLI S. & PASSERI L. (1991) - *Eteropie di facies nel Trias superiore e nel Lias inferiore del Gran Sasso.* Studi Geol. Camerti, Vol. Spec. (1991/2): 115-118.

BRUNI F., CALAMITA F., MARANCI M. & PIERANTONI P.P. (1996) - *Il controllo della tettonica giurassica sulla strutturazione neogenica dei Monti Martani meridionali (Preappennino umbro).* Studi Geol. Camerti, Vol. Spec., 1995/**1**: 121-135.

BOYER S.E., & ELLIOT D. (1982) - *Thrust systems.* Am. Ass. Petrol. Geol. Bull., **66**: 1196-1230.

BUTLER R.W.H. (1989) - *The influence of pre-existing basin structure on thrust system evolution in the Western Alps.* In: M.A. COOPER, & G.D. WILLIAMS, Inversion Tectonics (Eds). Geol. Soc., Spec. Publ., **44**: 105-122.

CALAMITA F., SCISCIANI V., MONTEFALCONE R., PALTRINIERI W. & PIZZI A. (2002) - *L'ereditarietà del paleomargine dell'Adria nella geometria del sistema orogenico centro appenninico: l'area abruzzese esterna.*

Memorie Società Geologica Italiana, **57**: 355-368.

CALAMITA F., PELOROSSO M. & SATOLLI S. (2003) - *Il ruolo dell'architettura del paleomargine mesozoico di Adria nel sistema orogenico del Gran Sasso d'Italia (Appennino Centrale).* Boll. Soc. Geol. It., **122**: 337-349.

CENTAMORE E., CANTALAMESSA G., MICARELLI A., POTETTI M., BERTI D., BIGI S., MORELLI C. & RIDOLFI M. (1991) - *Stratigrafia ed analisi di facies dei depositi del Miocene e del Pliocene inferiore dell' avanfossa marchigiano abruzzese e delle zone limitrofe.* Studi Geol. Camerti, Vol. Spec. (1991/**2**): 125-131.

COLTORTI M.& PIERUCCINI P. (2000) - *The planation surface across the Italian peninsula: a key tool in neotectonics studies.* J. of Geodynamics, **29**: 323-328.

COWARD M.P., DE DONATIS M., MAZZOLI S., PALTRINIERI W & WEZEL F.C. (1999) - *Frontal part of the northern Apeninnes fold and thrust belt in the Romagna-Marche area (Italy): shallow and deep structural styles.* Tectonics, **18** (3): 559-574.

DE LA PIERRE F., GHISETTI F., LANZA R. & VEZZANI L. (1992) - *Paleomagnetic and structural evidence of Neogene tectonic rotation of the Gran Sasso range (Central Apennines Italy).* Tectonophysics, **215**: 335-348.

GHISETTI F. & VEZZANI L. (1986) - *Assetto geometrico ed evoluzione strutturale della catena del Gran Sasso tra Vado di Siella e Vado di Corno.* Boll. Soc. Geol. It., **105**: 131-171.

GHISETTI F. & VEZZANI L. (1990) - *Stili strutturali nei sistemi di sovrascorrimento della catena del Gran Sasso /Appennino Centrale).* Studi Geol. Camerti, Vol. Spec., 37-50.

GHISETTI F. & VEZZANI L. (1991) - *Thrust belt development in the Central Apennines (Italy): northward polarity of thrusting and out-of-sequence deformations in the Gran Sasso chain.* Tectonics, **10**: 904-919.

GHISETTI F., VEZZANI L., BIGOZZI A., BLUMETTI A.M., BRUZZONE B., CELLINI M., CENTAMORE E., CLARI P., DE LA PIERRE F., FOLLADOR U., FREZZOTTI M., GIRAUDI C., PITTORI C. & RIDOLFI M. (1990) - *Carta geologica del*

Gran Sasso d'Italia da Vado di Corno al Passo delle Capannelle. Scala 1: 25.000, S.EL.CA. Firenze.

GIRAUDI C. & FREZZOTTI F. (1995) - *Paleosismicity in the Gran Sasso massif (Abruzzo Central Italy).* Quaternary International, **25**: 81-93.

GILLCRIST R., COWARD M.P., TRUDGILL B., PECHER A. & MUGNIER J.L. (1989) - *Structural inversion in the external French Alps.* In: M.A. COOPER & G.D. WILLIAMS, Inversion Tectonics (Eds). Geol. Soc., Spec. Publ., **44**: 354.

HOSSACK J.R. (1983) - *A cross-section through the Scandinavian Caledonides constructed with the aid of branch-line maps.* J. Struct. Geol, **5**: 103-111.

McCLAY K.R. (1989) - *Analogue models of inversion tectonics.* Geol. Soc., Spec. Publ., **44**: 41-59.

PIZZI A., CALAMITA F., COLTORTI M. & PIERUCCINI P. (2002) - *Quaternary normal faults, intramontane basins and seismicity in the Umbria-Marche-Abruzzi Apennine Ridge (Italy): contribution of neotectonic analysis to seismic hazard assessment.* Boll. Soc. Geol. It., Vol. spec. **1**: 923-929.

SCISCIANI V., CALAMITA F., TAVARNELLI E., RUSCIADELLI G., ORI G.G. & PALTRINIERI W. (2001) - *Foreland-dipping normal fault in the inner edges of syn-orogenic basin: A case in the Central Apennines.* Tectonophysics, **330**: 211-224.

SPERANZA F., ADAMOLI L. & MANISCALCO R. (2001) - *Genesi ed evoluzione del Fronte Arcuato del Gran Sasso: nuovi dati paleomagnetici.* Abstract 3° Convegno FIST, Settembre 2001, Chieti.

TAVARNELLI E. (1996) - *The effects of pre-existing normal faults on thrust ramp development: an example from the northern Apennines, Italy.* Geol. Rundsch., **85**: 363-371.

VAN KONIJNENBURG J.H., BERNULLI D. & MUTTI M. (1999) - *Stratigraphic architecture of a Lower Cretaceous-Lower Tertiary carbonate base-of-slope succession: Gran Sasso d'Italia (Central Apennines, Italy).* Society for Sedim. Geol., Spec. Publ., 291-315.

WELBON A. (1988) - *The influence of intrabasinal faults on the development of a linked thrust system.* Geol. Rundsch., **77**: 1-11.